Anisotropy-Induced Soliton Excitation in Magnetized Strong-Rung Spin Ladders

Yu. V. Krasnikova,[1,2,*] S. C. Furuya,[3] V. N. Glazkov,[1,2] K. Yu. Povarov,[4] D. Blosser,[4] and A. Zheludev[4]
[1]P. L. Kapitza Institute for Physical Problems, RAS, Kosygina 2, 119334 Moscow, Russia
[2]Laboratory for Condensed Matter Physics, National Research University Higher School of Economics, Myasnitskaya street 20, 101000 Moscow, Russia
[3]Condensed Matter Theory Laboratory, RIKEN, Wako, Saitama 351-0198, Japan
[4]Laboratory for Solid State Physics, ETH Zürich, 8093 Zürich, Switzerland

(Received 5 February 2020; revised 5 June 2020; accepted 23 June 2020; published 9 July 2020)

We report low temperature electron spin resonance experimental and theoretical studies of an archetype $S = 1/2$ strong-rung spin ladder material $(C_5H_{12}N)_2CuBr_4$. Unexpected dynamics is detected deep in the Tomonaga-Luttinger spin liquid regime. Close to the point where the system is half-magnetized (and believed to be equivalent to a gapless easy plane chain in zero field) we observed orientation-dependent spin gap and anomalous g-factor values. Field theoretical analysis demonstrates that the observed low-energy excitation modes in magnetized $(C_5H_{12}N)_2CuBr_4$ are solitonic excitations caused by Dzyaloshinskii-Moriya interaction presence.

DOI: 10.1103/PhysRevLett.125.027204

Understanding quantum many-body systems has always been a challenge. However, some exact solutions can be found for 1D systems [1]. There is a rich variety of low-dimensional magnets that could be approached in terms of Tomonaga-Luttinger spin liquid [2–4]. One of the simplest and well-described models for demonstrating the presence of Tomonaga-Luttinger spin liquid state (TLSL) is a two-leg spin ladder [5–7]. Such a system has a gap in energy spectrum below the first critical field and is expected to have gapless spectrum in TLSL phase above the first critical field B_{c1} up to the saturation field B_{c2} [8,9]. Moreover, mapping of the strong-rung spin ladder onto the exactly soluble XXZ spin chain can be realized in region between B_{c1} and B_{c2} [10–13].

In the real systems anisotropic spin interactions are always present. They typically lead to significant low energy spectrum changes [14–18]. Incorporating effects of such perturbations in TLSL description is one of the challenges in the research on 1D magnetic systems. However, not so many experimental methods allow to study the anisotropy induced effects in detail. Electron spin resonance spectroscopy (ESR) is perfectly suitable for this goal as it routinely allows energy resolution ~0.005 meV at $q = 0$.

In this Letter we report experimental and theoretical ESR studies for an archetype strong rung spin ladder model material $(C_5H_{12}N)_2CuBr_4$ (called BPCB) [6,12,19,20]. At low temperatures around the field corresponding to half-saturation of BPCB (i.e., deep in the TLSL regime) we found a gapped spectrum with unusual frequency-field dependencies. The conventional Heisenberg spin Hamiltonian of BPCB does not capture this behavior, as it predicts a complete softening of $q = 0$ excitations near the half-saturation field. Field theoretical analysis shows that the symmetry allowed pattern of Dzyaloshinskii-Moriya interaction (which can be accompanied by symmetric anisotropic exchange interactions) results in formation of low energy solitons in the spectrum of BPCB. The predicted field dependencies match the experimental results well and the gap variation with the field direction fixes the orientation of Dzyaloshinskii-Moriya vectors.

The material BPCB, crystallizing in a $P2_1/c$ monoclinic space group [21], represents an almost ideal $S = 1/2$ strong rung spin ladder model. The Cu^{2+} magnetic ions form a "rung" $S = 1/2$ dimer pairs with coupling $J_\perp \simeq 12.7$ K. Each dimer hosts an inversion center in the middle. The dimers are in turn coupled into ladders by the interaction $J_\parallel \simeq 3.54$ K (Fig. 1). In zero magnetic field this results in a quantum disordered singlet ground state with the gapped "triplon" $S = 1$ magnetic excitations, the gap value being

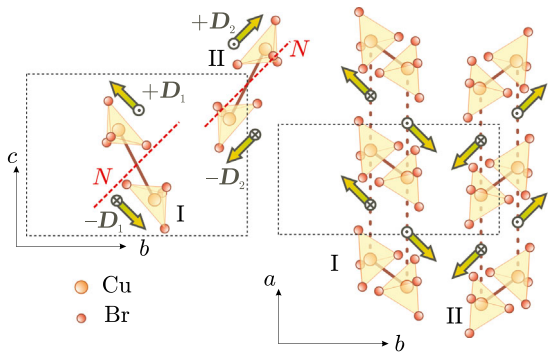

FIG. 1. Schematic representation of BPCB crystal structure. I and II mark two types of ladders, $\mathbf{D}_1$, $\mathbf{D}_2$: DM vectors directions, dashed line marks the N direction as described in the text.

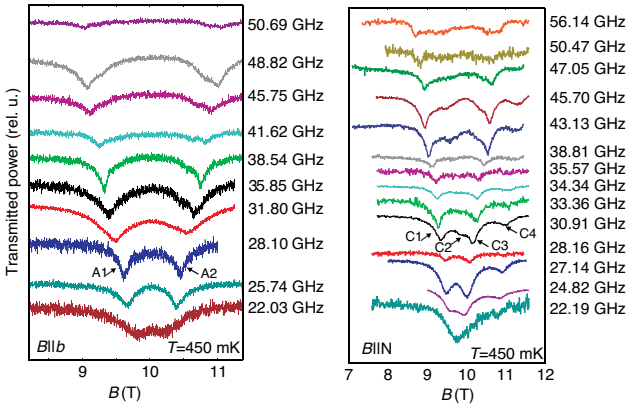

FIG. 2. ESR absorption spectra at $T = 450$ mK at different microwave frequencies. Left panel: magnetic field orientation $B\|b$. Right panel: magnetic field orientation $B\|N$. A1, A2, C1, C2, C3, C4 mark different ESR absorption components for both orientations.

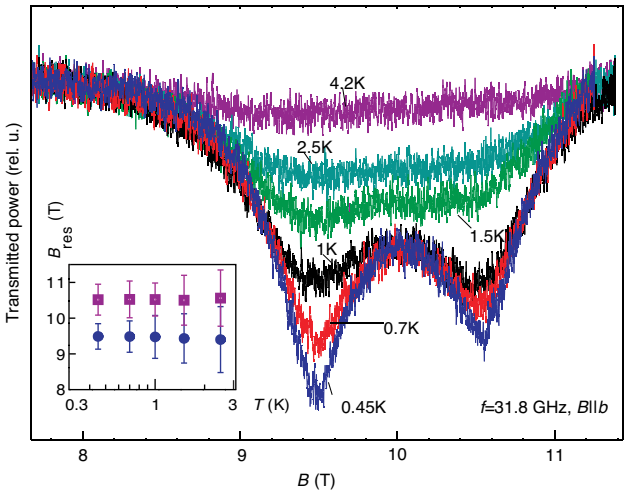

FIG. 3. Temperature dependence of ESR absorption signal for $\nu = 31.8$ GHz, sample orientation corresponds to $B\|b$. Inset: resonance field temperature dependence for both ESR absorption components, circles—left component, squares—right component. Vertical bars show *full* ESR linewidths at halfheight for both components.

$\Delta_{ZF} \simeq 9.2$ K. Between the gap closing field $B_{c1} = 6.6$ T and the saturation field $B_{c2} = 13.6$ T [11,20] the antiferromagnetic order exists below $T \simeq 0.1$ K. Above this threshold temperature it is replaced by a strongly correlated TLSL state, persisting up to 1.5 K [22]. Importantly, BPCB has two types of identical ladders oriented differently. They are equivalent for the field direction $B\|b$, and are most inequivalent for $B\|(bc)$ at 45° from the b axis [23,24]. This special orientation is denoted $B\|N$. Low symmetry of BPCB also allows anisotropic Dzyaloshinskii-Moriya (DM) interaction on the ladder legs. The DM vector **D** is uniform along the leg, is directed oppositely on two legs of the same ladder and is related by reflection symmetry in the adjacent ladders. No further constrains for its direction are present.

The multifrequency ESR spectra have been recorded in the Kapitza Institute in a custom-made spectrometer equipped with ^{3}He cryostat and 14 T cryomanget. The $m \approx 100$ mg deuterated BPCB crystal (from the same batch as in Refs. [23,25]) was placed in the cylindric microwave resonant cavity and the field dependent transmission spectra were recorded at the cavity eigenfrequencies. Two principal magnetic field directions, $B\|b$ and $B\|N$ were used. The data were collected well above the ordered state: from $T = 0.45$ to 20 K in a wide field range.

At $T > 10$ K we observed normal paramagnetic resonance with the g-factor values 2.18 for $B\|b$, 2.04 and 2.29 for $B\|N$, which are close to the previously reported values [21,24]. On cooling below $T \simeq \Delta_{ZF}$ this signal loses intensity and splits, as expected for ESR of thermally activated triplet excitations [15,24,26,27].

Besides this triplon-related low field absorption, we have detected a novel signal between two critical fields $B_{c1} = 6.6$ T and $B_{c2} = 13.6$ T at 450 mK (see Fig. 2). This signal exists in a broad frequency range and looses intensity on heating (see Fig. 3). Therefore we can state that the observed modes are solely low-temperature phenomenon and they are connected with presence of TLSL phase in BPCB. We highlight that the temperature of our experiment is well above the ordering temperature. This allows to neglect interladder coupling in further analysis.

Experimentally determined frequency-field diagrams are shown in Fig. 4. They were fitted by equation:

$$2\pi\hbar\nu = \sqrt{\Delta^2 + [(g_{\text{eff}}\mu_B(B - B^*)]^2}, \qquad (1)$$

fit parameters are shown in Fig. 4. The gap $\Delta/(2\pi\hbar)$ depends on magnetic field orientation varying from 14 to

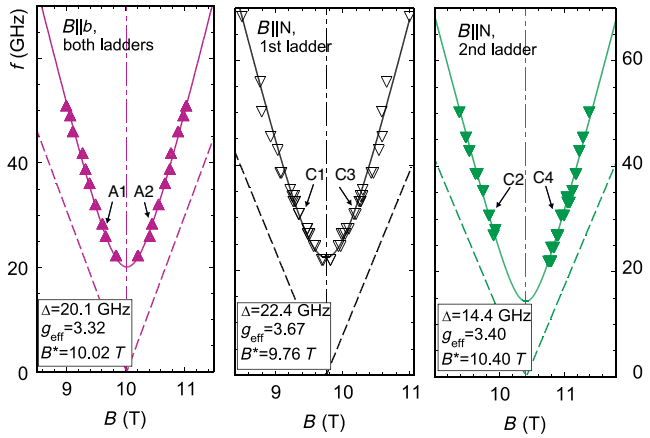

FIG. 4. Frequency-field dependencies for both studied orientations $B\|N$ and $B\|b$ at $T = 450$ mK. Symbols—experimental data, solid curves—fit by Eq. (1), dashed lines—isotropic model with experimentally measured g factors. A1, A2, C1, C2, C3, and C4 mark different ESR absorption components for both orientations. The errorbars are within the symbol size.

22 GHz for the orientations studied. Effective g-factor values vary from 3.2 to 3.7 for different field directions and are strongly renormalized compared to the bare values quoted above.

The presence of the anisotropic gap and the renormalization of effective g factor are not captured by a simple Heisenberg Hamiltonian:

$$\hat{\mathcal{H}} = \sum_j J_\perp \hat{\mathbf{S}}_{j,1}\hat{\mathbf{S}}_{j,2} + J_\parallel(\hat{\mathbf{S}}_{j,1}\hat{\mathbf{S}}_{j+1,1} + \hat{\mathbf{S}}_{j,2}\hat{\mathbf{S}}_{j+1,2}) - g\mu_B\mathbf{B}(\hat{\mathbf{S}}_{j,1} + \hat{\mathbf{S}}_{j,2}), \tag{2}$$

with index j runs along the ladder sites, and second index enumerates the ladder legs.

For $J_\perp \gg J_\parallel$, all the low energy properties of ladder (2) at $B > B_{c1}$ will essentially be defined by the two lowest energy states of the dimer on the rung of the ladder. This validates a "ladder-to-chain" mapping (see Ref. [12] and references therein):

$$\hat{S}_1^{x,y} = -\frac{\hat{T}^{x,y}}{\sqrt{2}}, \qquad \hat{S}_2^{x,y} = \frac{\hat{T}^{x,y}}{\sqrt{2}}, \qquad \hat{S}_1^z = \hat{S}_2^z = \frac{1+2\hat{T}^z}{4}. \tag{3}$$

Here, $\hat{T}^\alpha$ are the pseudospin operators that commute just like the normal spin operators. Assuming that z is the field direction, the transformed Hamiltonian becomes the one of an easy plane pseudospin-1/2 chain:

$$\hat{\mathcal{H}}_{XXZ} = \sum_j J_\parallel\left(\hat{T}_j^x\hat{T}_{j+1}^x + \hat{T}_j^y\hat{T}_{j+1}^y + \frac{1}{2}\hat{T}_j^z\hat{T}_{j+1}^z\right) - g\mu_B\left(B - \frac{J_\perp + J_\parallel/2}{g\mu_B}\right)\hat{T}_j^z \tag{4}$$

At a special magnetic field value $g\mu_B B^* = J_\perp + J_\parallel/2$ the system becomes equivalent to a nonmagnetized easy plane chain. Thus, theoretical model [12,13] predicts softening of $q = 0$ excitations at $B^* = (B_{c1} + B_{c2})/2$. Away from this point excitations spectrum should follow $2\pi\hbar\nu = g\mu_B|B - B^*|$.

Our observations are clearly inconsistent with this idealized Heisenberg model. This urges us to consider the effect of peculiar type of Dzyaloshinskii-Moriya interaction (uniform along the leg, opposite on different legs) present in BPCB:

$$\hat{\mathcal{H}}' = \sum_j \mathbf{D}[\hat{\mathbf{S}}_{j,1} \times \hat{\mathbf{S}}_{j+1,1}] - \mathbf{D}[\hat{\mathbf{S}}_{j,2} \times \hat{\mathbf{S}}_{j+1,2}]. \tag{5}$$

The Dzyaloshiniskii-Moriya vector $\mathbf{D} = (D_x, 0, D_z)$ may have both longitudinal and transverse components with respect to the external field. Under the transformation (3) the longitudinal part vanishes, and the transformed DM Hamiltonian becomes:

$$\hat{\mathcal{H}}'_{XXZ} = \frac{D_x}{\sqrt{2}}\sum_j(\hat{T}_j^y\hat{T}_{i+1}^z - \hat{T}_j^z\hat{T}_{j+1}^y). \tag{6}$$

This means that our effective model is now the one of a spin chain with uniform DM interaction. Heisenberg spin chains with this type of interaction are known to demonstrate gapped ESR spectra at zero magnetic field [17,28,29]. This would, in principle, explain the observed nonvanishing gap at field B^*. The present case, however, is strongly non-Heisenberg in terms of pseudospin and the effective DM interaction is perpendicular to the field direction z.

According to Kaplan-Shekhtman-Entin-Wohlman-Aharony (KSEA mechanism) [30,31], the possible D_x term should also be accompanied by a weak symmetric anisotropy term on the same bond:

$$\hat{\mathcal{H}}'' = \delta_x\sum_j \hat{S}_{j,1}^x\hat{S}_{j+1,1}^x + \hat{S}_{j,2}^x\hat{S}_{j+1,2}^x.$$

This is another possible source of nonvanishing gap at the "compensation field" B^*. After the transformation it becomes:

$$\hat{\mathcal{H}}''_{XXZ} = \delta_x\sum_j \hat{T}_j^x\hat{T}_{j+1}^x. \tag{7}$$

Actually, both $\hat{\mathcal{H}}'_{XXZ}$ and $\hat{\mathcal{H}}''_{XXZ}$ yield effectively the same relevant interaction responsible for the generation of the gap [7]. We have checked that δ_z component of KSEA generated by D_z does not contribute to the gap since it does not break the U(1) symmetry around the field direction z. The effective spin chain Hamiltonian [(4), (6), (7)] can be bosonized using the standard methods [1,7,12]. This yields the effective low-energy field theory near $B \approx B^*$ in the form of sine-Gordon-type Hamiltonian,

$$\hat{\mathcal{H}}_{\text{eff}} = \frac{v}{2\pi}\int dx\left[K\left(\frac{\partial\phi}{\partial x}\right)^2 + \frac{1}{K}\left(\frac{\partial\theta}{\partial x}\right)^2\right] + \lambda\int dx\cos(2\theta). \tag{8}$$

ϕ and θ are bosonic fields and are noncommutative with each other. K represents the strength of interactions and is called the Luttinger parameter [1]. The coupling constant λ is proportional to $(D_x/J_\parallel)^2$ for the following reason. The DM interaction (6) directly yields a complex interaction, $\cos\theta\sin(2\phi)$. This interaction itself is negligible in the low-energy Hamiltonian, but it generates the excitation gap indirectly by yielding the relevant interaction $\cos(2\theta)$ through a second-order perturbative process to the TLSL [7]. This indirect generation of $\cos(2\theta)$ can be regarded as the effective generation of the symmetric exchange anisotropy (7) [32] by the DM interaction (6).

The cosine interaction potential $\cos(2\theta)$ pins the θ field to one of its minima in the ground state. The pinning is

accompanied by a spontaneous breaking of the translation symmetry $\hat{\boldsymbol{T}}_j \to \hat{\boldsymbol{T}}_{j+1}$. One of the ground states has a transverse staggered magnetization $\langle \sum_j (-1)^j \hat{T}_j^x \rangle > 0$ and the other has $\langle \sum_j (-1)^j \hat{T}_j^x \rangle < 0$. Once the system chooses one of the doubly degenerate ground states spontaneously, its effective field theory (8) is reduced to be that of quantum spin chains in a transverse staggered field [7,16,33–35].

Magnetic excitations generated by ϕ and θ fields were closely investigated in the context of ESR [33,35]. Applying those ESR theories to BPCB, we conclude that our ESR measurements captured a single soliton (or an antisoliton) excitations at low temperatures. The soliton and the antisoltion are topological excitations that cause a tunneling of θ from one minimum of the cosine potential to another one [36]. In a magnetic field $B \approx B^*$, the pseudospin is bosonized as

$$\hat{T}_j^+ = e^{-i\theta}\left[(-1)^j B^* + b_1 \cos\left(2\phi + 2Kg\mu_B(B-B^*)\frac{x}{v\hbar}\right)\right], \tag{9}$$

where B^* and b_1 are nonuniversal constants [1,18]. The θ field is pinned to a constant and an operator $\exp[2i\phi(x)]$ generates a soliton at a position x. ESR thus detects a delta-function-like peak at a frequency [37]:

$$2\pi\hbar\nu = \sqrt{M^2 + [2Kg\mu_B(B-B^*)]^2}, \tag{10}$$

which corresponds to an excitation of a soliton [38,39] with the mass M, equal to the observed gap Δ, at an incommensurate wave number $q = 2Kg\mu_B(B-B^*)/(\hbar v)$ along the chain.

The effective g factor thus turns out to be

$$g_{\mathrm{eff}} = 2Kg. \tag{11}$$

Within the pseudospin approximation (4) the Luttinger parameter $K = 3/4$ at $B = B^*$ [1,40]. The theoretical prediction (11) is consistent with the observed anomalously large g factor including its field-orientation dependence. Taking into account higher orders of $J_\parallel/J_\perp$ expansion [12] one obtains for BPCB $K = 0.8$ (see details in [7]), which yields g-factor values close to the experimentally observed one (see Table I).

Unfortunately, it remains challenging to give a microscopic explanation to the field-orientation dependence of the soliton gap. This is because no microscopic information is available yet about the nonuniversal proportionality coefficient between the coupling constant λ and squares of DM vectors in general field orientations [7]. Still, one can ascertain that at $B\|N$ the soliton gap is decreasing as $|B-B^*|$ increases. This field dependence explains the reason why we observe the gapped soliton mode in ESR only in the small field range around $B = B^*$.

TABLE I. Comparison of experimentally measured g factors with the predictions of TLSL model.

	Experiment		TLSL theory [Eq. (11)]
	g ($T > 10$ K)	g_{eff} ($T = 0.45$ K)	
$B\|b$	2.18 ± 0.01	3.32 ± 0.05	3.49
$B\|N$	2.29 ± 0.02	3.67 ± 0.07	3.66
$B\|N$	2.04 ± 0.02	3.40 ± 0.05	3.26

We note that breather modes, which are bound states of the soliton and the antisoliton, are formed but invisible in ESR experiment because of a mismatch of wave numbers. The breather modes are developed near the wave number $q = \pi$ whereas ESR sees excitations at $q \approx 0$. A staggered DM interaction is requisite for rendering breathers observable in ESR [33,35] but it is forbidden in BPCB by the symmetry.

We also can estimate possible DM vector orientation from soliton gap values. From the bosonization theory, we know that $\Delta \propto (D_\perp)^{[4K/(4K-1)]}$, where K is the Luttinger parameter and $D_\perp$ is DM magnitude transverse to the magnetic field. DM vector directions in inequivalent ladders are linked by crystal symmetry. By taking ratios of ESR gaps and assuming $K = 0.8$ as follows from the TLSL model we obtained DM vector directions (see Fig. 1). Found projections of DM vectors on (bc) plane are practically the same as in Ref. [24], but our analysis predicts that DM vector component parallel to the ladder has approximately the same length as the component transverse to the ladder. Procedure of estimation is described in details in the Supplemental Material [7].

We also put special emphasis on the coexistence of the gapless TLSL behavior and the gapped soliton mode. This coexistence originates from differences of two types of spin ladders. The spin ladder has the finite soliton gap in a field range $B^* - \delta B \le B \le B^* + \delta B$, where δB corresponds to the soliton gap at $h_{\mathrm{eff}} = 0$ through $\delta B = M/(g_{\mathrm{eff}}\mu_B)$ [7]. We estimate from our experimental data that the first ladder has the soliton gap for $9.32\ \mathrm{T} \le B \le 10.2\ \mathrm{T}$ and the second ladder has the gap for $10.1\ \mathrm{T} \le B \le 10.7\ \mathrm{T}$. When the first ladder has the gap, the second ladder remains gapless in the TLSL phase, and vice versa. Both spin ladders are gapped simultaneously, if they could, in an invisibly narrow field range.

To summarize, this Letter illustrates how crucial the presence of anisotropy could be in the system as it leads to symmetry breaking and ground state changes. Gapped behavior of frequency-field dependencies indicates presence of massive modes at $q = 0$ in region where massless modes were expected. The DM vector that breaks the U(1) spin-rotation symmetry is responsible for the gapped mode. Our analysis with the DM vector is not only consistent with

a previous ESR theory of BPCB [32] but also provides more realistic microscopic model of BPCB. This untypical and unexpected behavior of energy spectra bridges theory and experiment and provides one more example of quantitative test of the TLSL model, leading to the deeper understanding of low-dimensional systems physics.

We thank Professor A. I. Smirnov, Professor L. E. Svistov, and T. A. Soldatov for helpful discussions. Samples were grown by evaporation method in ETH Zurich. ESR experiments were performed in P. L. Kapitza Institute. The experimental work was supported by Russian Science Foundation Grant No. 17-12-01505. Data analysis was supported by Program of fundamental studies of HSE. Work at ETHZ was supported by Swiss National Science Foundation, Division II.

*krasnikova.mipt@gmail.com

[1] T. Giamarchi, *Quantum Physics in One Dimension* (Clarendon, Oxford, 2003).

[2] S. Tomonaga, Remarks on Bloch's method of sound waves applied to many-fermion problems, Prog. Theor. Phys. **5**, 544 (1950); J. M. Luttinger, An exactly soluble model of a many-fermion system, J. Math. Phys. (N.Y.) **4**, 1154 (1963); D. C. Mattis and E. H. Lieb, Exact solution of a many-fermion system and its associated Boson field, J. Math. Phys. (N.Y.) **6**, 304 (1965).

[3] F. D. M. Haldane, General Relation of Correlation Exponents and Spectral Properties of One-Dimensional Fermi Systems: Application to the Anisotropic $S = 1/2$ Heisenberg Chain, Phys. Rev. Lett. **45**, 1358 (1980).

[4] T. Giamarchi, Some experimental tests of Tomonaga-Luttinger liquids, Int. J. Mod. Phys. B **26**, 1244004 (2012).

[5] M. Jeong, H. Mayaffre, C. Berthier, D. Schmidiger, A. Zheludev, and M. Horvatić, Attractive Tomonaga-Luttinger Liquid in a Quantum Spin Ladder, Phys. Rev. Lett. **111**, 106404 (2013); K. Yu. Povarov, D. Schmidiger, N. Reynolds, R. Bewley, and A. Zheludev, Scaling of temporal correlations in an attractive Tomonaga-Luttinger spin liquid, Phys. Rev. B **91**, 020406(R) (2015); M. Jeong, D. Schmidiger, H. Mayaffre, M. Klanjšek, C. Berthier, W. Knafo, G. Ballon, B. Vignolle, S. Krämer, A. Zheludev, and M. Horvatić, Dichotomy between Attractive and Repulsive Tomonaga-Luttinger Liquids in Spin Ladders, Phys. Rev. Lett. **117**, 106402 (2016).

[6] B. Thielemann, C. Rüegg, H. M. Rønnow, A. M. Läuchli, J.-S. Caux, B. Normand, D. Biner, K. W. Krämer, H.-U. Güdel, J. Stahn, K. Habicht, K. Kiefer, M. Boehm, D. F. McMorrow, and J. Mesot, Direct Observation of Magnon Fractionalization in the Quantum Spin Ladder, Phys. Rev. Lett. **102**, 107204 (2009).

[7] See the Supplemental Material at http://link.aps.org/supplemental/10.1103/PhysRevLett.125.027204 for theoretical details and ESR in strong-leg spin ladder compound in the Tomonaga-Luttinger spin liquid phase, which includes Ref. [8].

[8] T. M. Rice, S. Gopalan, and M. Sigrist, Superconductivity, spin gaps and Luttinger liquids in a class of cuprates, Europhys. Lett. **23**, 445 (1993).

[9] E. Dagotto, Experiments on ladders reveal a complex interplay between a spin-gapped normal state and superconductivity, Rep. Prog. Phys. **62**, 1525 (1999).

[10] G. Chaboussant, M.-H. Julien, Y. Fagot-Revurat, M. Hanson, L. P. Lévy, C. Berthier, M. Horvatić, and O. Piovesana, Zero temperature phase transitions in spin-ladders: Phase diagram and dynamical studies of $Cu_2(C_5H_{12}N_2)_2Cl_4$, Eur. Phys. J. B **6**, 167 (1998).

[11] B. C. Watson, V. N. Kotov, M. W. Meisel, D. W. Hall, G. E. Granroth, W. T. Montfrooij, S. E. Nagler, D. A. Jensen, R. Backov, M. A. Petruska, G. E. Fanucci, and D. R. Talham, Magnetic Spin Ladder $(C_5H_{12}N)_2CuBr_4$: High-Field Magnetization and Scaling near Quantum Criticality, Phys. Rev. Lett. **86**, 5168 (2001).

[12] P. Bouillot, C. Kollath, A. M. Läuchli, M. Zvonarev, B. Thielemann, C. Rüegg, E. Orignac, R. Citro, M. Klanjšek, C. Berthier, M. Horvatić, and T. Giamarchi, Statics and dynamics of weakly coupled antiferromagnetic spin-$\frac{1}{2}$ ladders in a magnetic field, Phys. Rev. B **83**, 054407 (2011).

[13] T. Giamarchi and A. M. Tsvelik, Coupled ladders in a magnetic field, Phys. Rev. B **59**, 11398 (1999).

[14] D. C. Dender, P. R. Hammar, D. H. Reich, C. Broholm, and G. Aeppli, Direct Observation of Field-Induced Incommensurate Fluctuations in a One-Dimensional $S = 1/2$ Antiferromagnet, Phys. Rev. Lett. **79**, 1750 (1997).

[15] V. N. Glazkov, A. I. Smirnov, H. Tanaka, and A. Oosawa, Spin-resonance modes of the spin-gap magnet $TlCuCl_3$, Phys. Rev. B **69**, 184410 (2004).

[16] S. A. Zvyagin, A. K. Kolezhuk, J. Krzystek, and R. Feyerherm, Excitation Hierarchy of the Quantum Sine-Gordon Spin Chain in a Strong Magnetic Field, Phys. Rev. Lett. **93**, 027201 (2004).

[17] K. Y. Povarov, A. I. Smirnov, O. A. Starykh, S. V. Petrov, and A. Y. Shapiro, Modes of Magnetic Resonance in the Spin-Liquid Phase of Cs_2CuCl_4, Phys. Rev. Lett. **107**, 037204 (2011).

[18] T. Hikihara and A. Furusaki, Correlation amplitudes for the spin-1/2 XXZ chain in a magnetic field, Phys. Rev. B **69**, 064427 (2004).

[19] B. Thielemann *et al.*, Field-controlled magnetic order in the quantum spin-ladder system $(Hpip)_2CuBr_4$, Phys. Rev. B **79**, 020408(R) (2009).

[20] M. Klanjšek, H. Mayaffre, C. Berthier, M. Horvatič, B. Chiari, O. Piovesana, P. Bouillot, C. Kollath, E. Orignac, R. Citro, and T. Giamarchi, Luttinger liquid physics in the spin ladder material $(C_5H_{12}N)_2CuBr_4$, Phys. Status Solidi C **247**, 656 (2010).

[21] B. R. Patyal, B. L. Scott, and R. D. Willett, Crystal-structure, magnetic-susceptibility, and EPR studies of bis (piperidinium)tetrabromocuprate(II): A novel monomer system showing spin diffusion, Phys. Rev. B **41**, 1657 (1990).

[22] C. Rüegg, K. Kiefer, B. Thielemann, D. F. McMorrow, V. Zapf, B. Normand, M. B. Zvonarev, P. Bouillot, C. Kollath, T. Giamarchi, S. Capponi, D. Poilblanc, D. Biner, and K. W. Krämer, Thermodynamics of the Spin Luttinger Liquid in a Model Ladder Material, Phys. Rev. Lett. **101**, 247202 (2008).

[23] D. Blosser, V. K. Bhartiya, D. J. Voneshen, and A. Zheludev, Origin of magnetic anisotropy in the spin ladder compound $(C_5H_{12}N)_2CuBr_4$, Phys. Rev. B **100**, 144406 (2019).

[24] E. Čižmár, M. Ozerov, J. Wosnitza, B. Thielemann, K. W. Krämer, C. Rüegg, O. Piovesana, M. Klanjšek, M. Horvatić, C. Berthier, and S. A. Zvyagin, Anisotropy of magnetic interactions in the spin-ladder compound $(C_5H_{12}N)_2CuBr_4$, Phys. Rev. B **82**, 054431 (2010).

[25] D. Blosser, V. K. Bhartiya, D. J. Voneshen, and A. Zheludev, $z = 2$ Quantum Critical Dynamics in a Spin Ladder, Phys. Rev. Lett. **121**, 247201 (2018).

[26] V. N. Glazkov, M. Fayzullin, Y. Krasnikova, G. Skoblin, D. Schmidiger, S. Mühlbauer, and A. Zheludev, ESR study of the spin ladder with uniform Dzyaloshinskii-Moriya interaction, Phys. Rev. B **92**, 184403 (2015).

[27] V. N. Glazkov, T. S. Yankova, J. Sichelschmidt, D. Hüvonen, and A. Zheludev, Electron spin resonance study of anisotropic interactions in a two-dimensional spin-gap magnet $(C_4H_{12}N_2)(Cu_2Cl_6)$, Phys. Rev. B **85**, 054415 (2012).

[28] A. I. Smirnov, T. A. Soldatov, K. Y. Povarov, M. Hälg, W. E. A. Lorenz, and A. Zheludev, Electron spin resonance in a model $S = 1/2$ chain antiferromagnet with a uniform Dzyaloshinskii-Moriya interaction, Phys. Rev. B **92**, 134417 (2015).

[29] T. A. Soldatov, A. I. Smirnov, K. Y. Povarov, M. Hälg, W. E. A. Lorenz, and A. Zheludev, Spin gap in the quasi-one-dimensional $S = 1/2$ antiferromagnet $K_2CuSO_4Cl_2$, Phys. Rev. B **98**, 144440 (2018).

[30] T. A. Kaplan, Single-band Hubbard model with spin-orbit coupling, Z. Phys. B **49**, 313 (1983); L. Shekhtman, O. Entin-Wohlman, and A. Aharony, Moriya's Anisotropic Superexchange Interaction, Frustration, and Dzyaloshinsky's Weak Ferromagnetism, Phys. Rev. Lett. **69**, 836 (1992); L. Shekhtman, A. Aharony, and O. Entin-Wohlman, Bond-dependent symmetric and antisymmetric superexchange interactions in La_2CuO_4, Phys. Rev. B **47**, 174 (1993).

[31] A. Zheludev, S. Maslov, I. Tsukada, I. Zaliznyak, L. P. Regnault, T. Masuda, K. Uchinokura, R. Erwin, and G. Shirane, Experimental Evidence for Kaplan–Shekhtman–Entin-Wohlman–Aharony Interactions in $Ba_2CuGe_2O_7$, Phys. Rev. Lett. **81**, 5410 (1998).

[32] S. C. Furuya, P. Bouillot, C. Kollath, M. Oshikawa, and T. Giamarchi, Electron Spin Resonance Shift in Spin Ladder Compounds, Phys. Rev. Lett. **108**, 037204 (2012).

[33] M. Oshikawa and I. Affleck, Electron spin resonance in $S = \frac{1}{2}$ antiferromagnetic chains, Phys. Rev. B **65**, 134410 (2002).

[34] I. Kuzmenko and F. H. L. Essler, Dynamical correlations of the spin-1/2 Heisenberg XXZ chain in a staggered field, Phys. Rev. B **79**, 024402 (2009).

[35] S. C. Furuya and M. Oshikawa, Boundary Resonances in $S = 1/2$ Antiferromagnetic Chains under a Staggered Field, Phys. Rev. Lett. **109**, 247603 (2012).

[36] Q. Faure, S. Takayoshi, S. Petit, V. Simonet, S. Raymond, L.-P. Regnault, M. Boehm, J. S. White, M. Månsson, C. Rüegg, P. Lejay, C. Benjamin, L. Thomas, S. C. Furuya, T. Giamarchi, and B. Grenier, Topological quantum phase transition in the Ising-like antiferromagnetic spin chain $BaCo_2V_2O_8$, Nat. Phys. **14**, 716 (2018).

[37] S. C. Furuya and T. Momoi, Electron spin resonance for the detection of long-range spin nematic order, Phys. Rev. B **97**, 104411 (2018).

[38] A. B. Zamolodchikov, Mass scale in the sine-Gordon model and its reduction, Int. J. Mod. Phys. A **10**, 1125 (1995).

[39] S. Lukyanov and A. Zamolodchikov, Form factors of soliton-creating operators in the sine-Gordon model, Nucl. Phys. **B607**, 437 (2001).

[40] D. C. Cabra, A. Honecker, and P. Pujol, Magnetization plateaux in n-leg spin ladders, Phys. Rev. B **58**, 6241 (1998).